Inorganic Chemistry

Article

pubs.acs.org/IC

# Abnormal Reduction, $Eu^{3+} \rightarrow Eu^{2+}$, and Defect Centers in $Eu^{3+}$-Doped Pollucite, $CsAlSi_2O_6$, Prepared in an Oxidizing Atmosphere

Hongde Xie,[†] Juan Lu,[†] Ying Guan,[†] Yanlin Huang,[†] Donglei Wei,[‡] and Hyo Jin Seo*[,‡]

[†]College of Chemistry, Chemical Engineering and Materials Science, Soochow University, Suzhou 215123, China

[‡]Department of Physics and Center for Marine-Integrated Biomedical Technology, Pukyong National University, Busan 608-737, Republic of Korea

**ABSTRACT:** Eu-doped pollucite $CsAlSi_2O_6$ was synthesized by the sol−gel method and heated in an air atmosphere. The crystal structure and the microstructure of the phosphors were investigated by X-ray powder diffraction and SEM images, respectively. The photoluminescence spectra and temperature dependent decay curves were measured. An abnormal reduction phenomenon of $Eu^{3+} \rightarrow Eu^{2+}$ was reported when $Eu^{3+}$ ions were doped in alkaline metal cation sites in $CsAlSi_2O_6$ prepared in an oxidizing atmosphere. The abnormal mechanism was discussed on the basis of the charge compensation model and a rigid three-dimensional framework structure of $CsAlSi_2O_6$. The luminescence color centers were investigated by luminescence decay lifetimes and thermal stabilities of $Eu^{2+}$ ions. The defect complexes of $[(Eu^{3+}{}_{Cs})^{\bullet\bullet}-2V_{Cs}{}']$ or $[(Eu^{3+}{}_{Cs})^{\bullet\bullet}-O_i{}'']$ induced by the substitution of $Eu^{3+}$ on $Cs^+$ were suggested in the lattices. $Eu^{2+}$ ions could be regarded as $Eu^{3+}$ ions combining with the released electrons from defects $O_i{}''$ or $V_{Cs}{}'$ in close vicinity of $Eu^{3+}$ ($Eu^{3+} + e$); the electrons cannot enter the atom track of $Eu^{2+}$ presenting luminescence of $Eu^{2+}$ ions. The results indicate that several defect traps can be attributed to the abnormal reduction mechanism of $Eu^{3+}$ to $Eu^{2+}$ ions in a matrix.

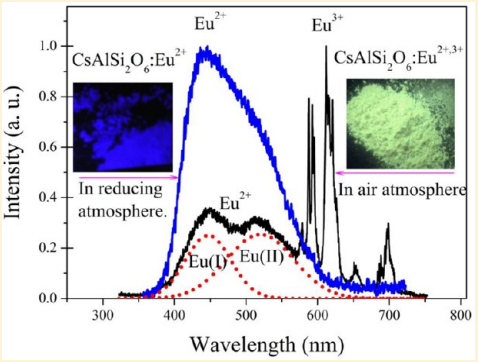


## 1. INTRODUCTION

Luminescence properties of divalent europium ion ($Eu^{2+}$)-activated materials have been investigated in many kinds of hosts for lighting and display due to their intense excitation, strong broad emission band, and tunable luminescence colors. It is well-known that there is no natural material containing $Eu^{2+}$ ions, so it is necessary to reduce $Eu^{3+}$ to $Eu^{2+}$ in a host. Usually this can be realized in a matrix if preparations are carried out in reducing atmospheres, such as $H_2$, $H_2/N_2$, or CO.

However, it is interesting that in some special compounds a reduction of trivalent rare earth ions ($RE^{3+}$; RE = $Sm^{3+}$, $Eu^{3+}$, or $Yb^{3+}$) into divalent ions $RE^{2+}$ ($Sm^{2+}$, $Eu^{2+}$, or $Yb^{2+}$) could happen even when samples were prepared in air at high temperature. Up to now, this "abnormal" reduction phenomenon, $RE^{3+} \rightarrow RE^{2+}$ in an oxidizing atmosphere, has been observed in the following hosts: borates ($SrB_4O_7$,[1] $SrB_6O_{10}$,[2] $BaB_8O_{13}$,[1] or $CaB_2O_4$[3]), haloborate ($Sr_2B_5O_9Cl$),[4,5] aluminates ($Sr_4Al_{14}O_{25}$[6,7] or $BaAl_2O_4$[8]), phosphates ($Ba_3(PO_4)_2$[9] or $NaCaPO_4$[10]), borophosphates ($MBPO_5$, M = Ca, Sr, or Ba),[11,12] silicate ($BaMgSiO_4$),[13] sulfate ($BaSO_4$),[14] borophosphate glasses ($ZnO-B_2O_3-P_2O_5$),[15] and Eu/Al-codoped high silica glasses ($95.5SiO_2-4B_2O_3-0.5Na_2O$ (wt %)).[16] This "abnormal" reduction was found to happen only in a special compound with rigid three-dimensional (3-D) enclosed crystal structures, with tetrahedral groups such as tetrahedral $BO_4$, $SiO_4$, $AlO_4$, or $PO_4$ groups.[1]

As a well-known aluminosilicate framework compound, pollucite ($CsAlSi_2O_6$), is of considerable interest because it has relatively high resistance to alteration under hydrothermal conditions and, thus, can potentially be used as a solid host for radioactive cesium immobilization.[17−19] Pollucite has unique thermal expansion; hence, it is used as a component in high-temperature glass-ceramic materials.[20−22] In addition, natural pollucite, which commonly contains an analcime ($CsAlSi_2O_6-H_2O$) component and mainly occurs in rare-element granitic pegmatites, is the primary industrial source of cesium and is of petrogenetic interest as an indicator of the advanced stage in pegmatitic magma fractionation.[23,24] Synthesis,[25] structure, and thermochemical study,[26] storage of radionuclides,[27] and substitution of impurity ions[24] in $CsAlSi_2O_6$ have been reported in recent years. Very recently, Zhang et al.[28] reported luminescence properties of $Eu^{2+}$-doped $CsAlSi_2O_6$ phosphors: blue-green color with CIE coordinates of ($x$ = 0.21, $y$ = 0.32) and a quantum efficiency of 67%. The possible application as a white light emission diode (LED) phosphor was suggested on the base of its bright blue-green luminescence and thermal stability.

Pollucite ($CsAlSi_2O_6$) can provide a rigid framework with covalent surrounding for $RE^{2+}$ ion doping. In this work, we reported an abnormal reduction of $Eu^{3+} \rightarrow Eu^{2+}$ in pollucite, $CsAlSi_2O_6$, when the compound was prepared in air at high temperature. Photoluminescence excitation and emission together with decay curves were measured at different

**Received:** August 26, 2013
**Published:** December 24, 2013

   dx.doi.org/10.1021/ic402169w | *Inorg. Chem.* 2014, 53, 827−834

temperatures. The mechanism of this reduction was explained according to the charge compensation model and the rigid crystal structure. The color centers were first discussed on the basis of the luminescence properties and thermal stabilities of $Eu^{2+}$ luminescence.

## 2. EXPERIMENTAL SECTION

Eu-doped $CsAlSi_2O_6$ was prepared by the sol−gel method, which can give the highest possible homogeneity for the material. The doping level was 5.0 mol % according to the optimal doping value reported by Zhang et al.[28] The raw materials were a stoichiometric mixture of cesium nitrate ($CsNO_3$), $Al(NO_3)_3$, tetraethyl silicate ($Si(OC_2H_5)_4$, TEOS), $Eu_2O_3$, and citric acid as the chelating agent. Briefly, the nitrate−europium solution was obtained by dissolving $Eu_2O_3$ in the diluted $HNO_3$, which was mixed with $CsNO_3$ and $Al(NO_3)_3$ in an aqueous solution of citric acid (99.5%) under constant stirring at 60−80 °C until the clear solution "A" was obtained. Then TEOS was mixed with some diluted $HNO_3$ and ethanol. The mixtures were hydrolyzed for 30−60 min under stirring to form solution "B". Then, A and B were mixed together and stirred for several hours at room temperature. Ethylene glycol (ethylene glycol and citric acid in a 4:1 molar ratio) can be added to promote the polymerization of the metal citrates by the polyesterification reaction. The solutions were slowly heated up to 100 °C and kept at this temperature for 2 h. The obtained gels were put into an oven to dry at 100−150 °C for 10−20 h to produce the porous solid resins; then solid resins were treated in air at 600 °C for 3−5 h. After that, the sample was thoroughly mixed and heated at 1300 °C for 5−10 h in air. This sample can be denoted as $CsAlSi_2O_6$-A, hereafter. In a comparison, the sample $CsAlSi_2O_6$:$Eu^{2+}$ prepared by heating it in a thermal ($H_2$ + $N_2$)-reducing atmosphere was denoted as $CsAlSi_2O_6$-C.

The phase purity was checked by powder X-ray diffraction (XRD) analysis collected on a Rigaku D/Max diffractometer operating at 40 kV, 30 mA with Bragg−Brentano geometry using Cu K$\alpha$ radiation ($\lambda$ = 1.5405 Å). Scanning electron micrograph (SEM) images and electron-dispersive X-ray (EDX) were obtained using a JEOL JSM-6360 LA instrument. In this measurement, the powder samples were fixed on the conductive adhesive and coated with Au thin film. Electron spin resonance (ESR) measurement was made on a Bruker A-300 spectrometer working at the X-band frequency. The photoluminescence excitation and emission spectra were recorded on a PerkinElmer LS-50B luminescence spectrometer. The luminescence decay was measured using the fourth harmonic (266 nm) of a pulsed Nd:YAG laser.

## 3. RESULTS AND DISCUSSION

**3.1. Crystal Phase Formation.** Figure 1 shows the XRD profiles of the $CsAlSi_2O_6$-A sample sintered in air and $CsAlSi_2O_6$-C in a thermal ($H_2$ + $N_2$)-reducing atmosphere. The XRD diffraction peaks on the patterns can be well indexed according to the PDF2 standard card number No. 29-0407 ($CsAlSi_2O_6$) selected in the International Centre for Diffraction Data (ICDD) database. The two samples are all in the pure $CsAlSi_2O_6$ phase except for a few tiny extra diffraction peaks, which are in permitted limit.

Figure 2 shows the representative SEM micrograph of Eu-doped $CsAlSi_2O_6$ prepared in air (1300 °C for 7 h). The sample shows close packed and well-grown grains. The particles have very fine and irregular elliptical or ball shapes with an average size of 1−2 $\mu$m.

Figure 3a,b shows the SEM images of $CsAlSi_2O_6$-A and $CsAlSi_2O_6$-C, respectively, in a low magnification. There is aggregation of the particles. Energy-dispersive X-ray (EDX) spectroscopy was used to examine the elemental compositions. The representative EDX spectra of the selected samples of $CsAlSi_2O_6$-A and $CsAlSi_2O_6$-C are shown in Figure 3c,d,

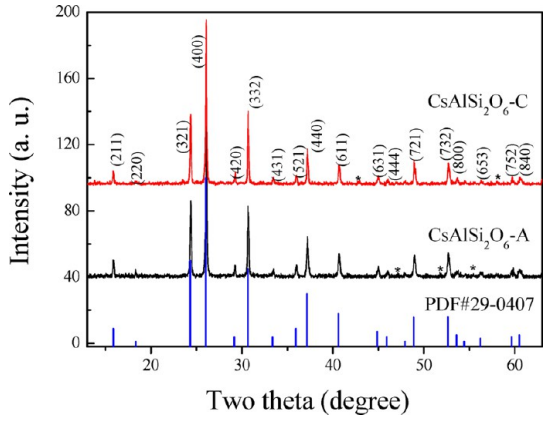


**Figure 1.** XRD patterns of Eu-doped $CsAlSi_2O_6$ prepared in air ($CsAlSi_2O_6$-A) and reducing atmosphere ($CsAlSi_2O_6$-C) in comparison with standard card PDF29-0407. The asterisk denotes some tiny extra diffraction peaks.

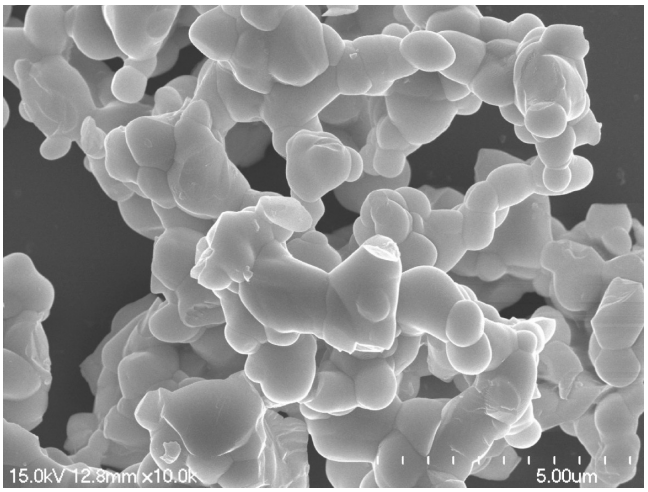


**Figure 2.** SEM micrograph of Eu-doped $CsAlSi_2O_6$ prepared in air (1300 °C for 7 h). The sample shows close packed and well-grown grains. The particles have very fine and irregular elliptical or ball shapes with an average size of 1−2 $\mu$m.

respectively. Several specific lines on the EDX spectra show the signals of Cs, Al, Si, O, and Eu, elements in the prepared samples. No the other elements such as carbon can be detected, which could remain in the intermediate stages (referred to as solid resins) because the sol−gel synthetic route was used for the samples. The quantitative ratio for the different elements is listed in the insets in Figure 3. The EDX spectra confirm the presence of Cs, Al, Si, O, and Eu, and the approximate surface compositions of Cs, Al, and Si, extracted from the EDX analysis, are much closer to the theoretical value in $CsAlSi_2O_6$. The amount of $Eu^{3+}$ obtained by EDX analysis in $CsAlSi_2O_6$-A and $CsAlSi_2O_6$-C was 1.48 and 1.65 atom %, respectively. The calculated values are lower than those in the precursors, but it can confirm $Eu^{3+}$ doping in the lattices.

**3.2. Photoluminescence Properties.** It has been established that $4f^65d \rightarrow 4f^7$ emission transitions of $Eu^{2+}$ in a compound are allowed, resulting in broad luminescence spectra and a very short lifetime in nanosecond to microsecond regions.[29,30] $Eu^{3+}$ ions show typical emission lines the spectral region of 570−725 nm corresponding $^5D_0$−$^7F_J$ ($J$ = 0−4) transitions with a lifetime longer than several milliseconds. So


dx.doi.org/10.1021/ic402169w | Inorg. Chem. 2014, 53, 827−834

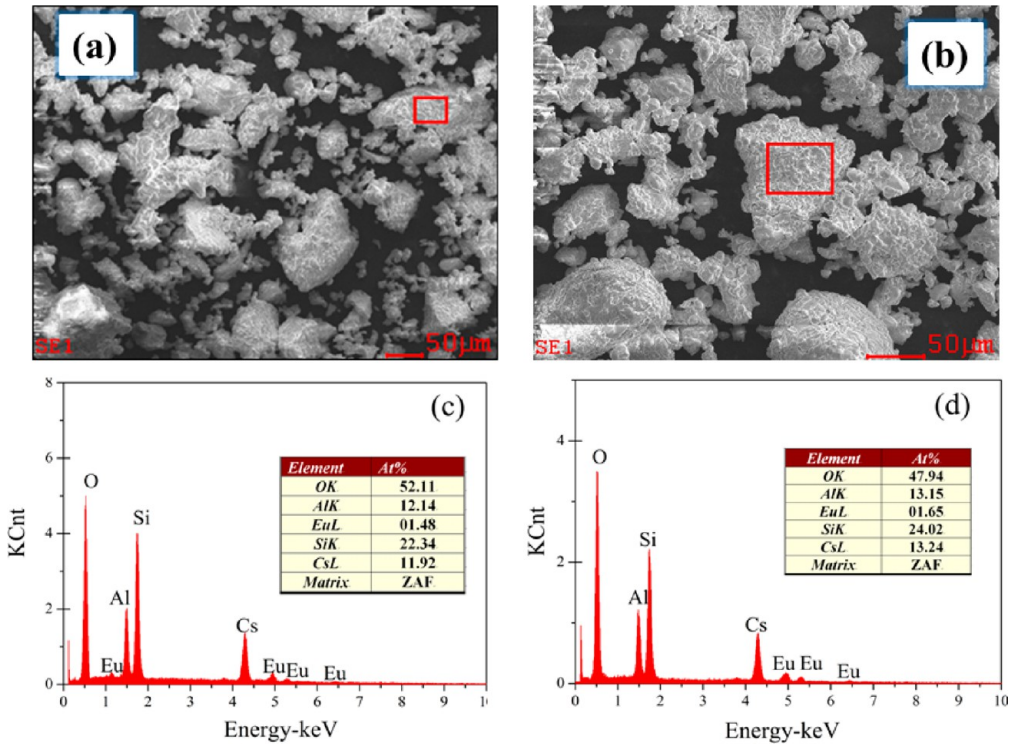


**Figure 3.** SEM images of $CsAlSi_2O_6$-A (a) and $CsAlSi_2O_6$-C (b) prepared at 1300 °C and (c, d) element EDX analysis of $CsAlSi_2O_6$-A and $CsAlSi_2O_6$-C, respectively. Insets show the quantitative ratio of the elements calculated from EDX data.

$Eu^{2+}$ and $Eu^{3+}$ can be well separated by very distinct spectra and luminescence decay curves (lifetimes).

The emission spectra of $CsAlSi_2O_6$:Eu prepared in air ($\lambda_{ex}$ = 300 nm, $\lambda_{ex}$ = 395 nm) are shown in Figure 4. The emission

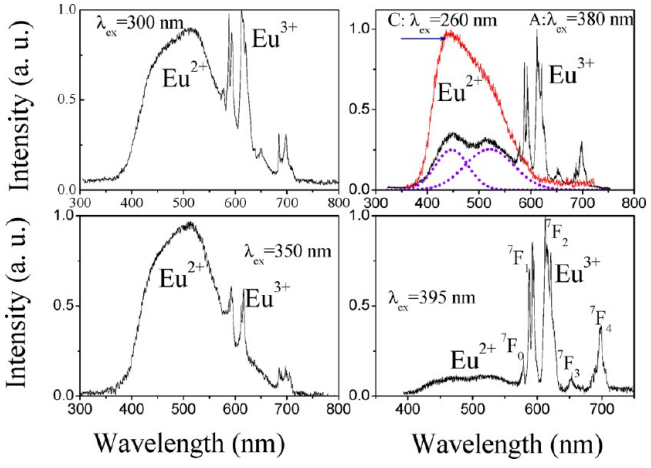


**Figure 4.** Emission spectra of $CsAlSi_2O_6$:Eu-A prepared in air ($\lambda_{ex}$ = 300, 350, 380, and 395 nm). Luminescence peaks from $^5D_0$ states of $Eu^{3+}$ are labeled. The emission spectrum of $CsAlSi_2O_6$:$Eu^{2+}$ prepared in reducing atmosphere ($CsAlSi_2O_6$-C) ($\lambda_{ex}$ = 260 nm) was added for a comparison.

spectra present the broad band (350−600 nm) and sharp emission peaks. The emission peaks in the range from 570 to 650 nm clearly belong to the f−f transitions of $^5D_0$−$^7F_J$ ($J$ = 0, 1, 2, 3, and 4) of $Eu^{3+}$. Since the nondoped sample of $CsAlSi_2O_6$ does not show any light, the broad emission bands at 350 and 600 nm could be from the emissions of $Eu^{2+}$ ions.

To identify the $Eu^{2+}$ ions in $CsAlSi_2O_6$:Eu prepared in air, the emission spectrum of $CsAlSi_2O_6$:$Eu^{2+}$ prepared in a thermal ($H_2$ + $N_2$)-reducing atmosphere ($CsAlSi_2O_6$-C) is shown in Figure 4 (C, $\lambda_{ex}$ = 260 nm). By comparing the spectral characteristics of the emission bands in two samples, it is easily seen that the shapes and positions of the emission bands are almost the same. The same broad emission bands of $Eu^{2+}$ ion in $CsAlSi_2O_6$ were situated from 350 to 600 nm, which were reported by Zhang et al.;[28] there are two emission bands at 440 and 530 nm with respective lifetimes of 1.18 and 2.76 $\mu$s. By the time-resolved spectra, the $Eu^{3+}$ luminescence can be distinctly separated from $Eu^{2+}$ as displayed in Figure 5. The emission spectra under short delay time show a dominate band from $Eu^{2+}$. Under the time delay, 100 $\mu$s, the emission transitions $^5D_0$

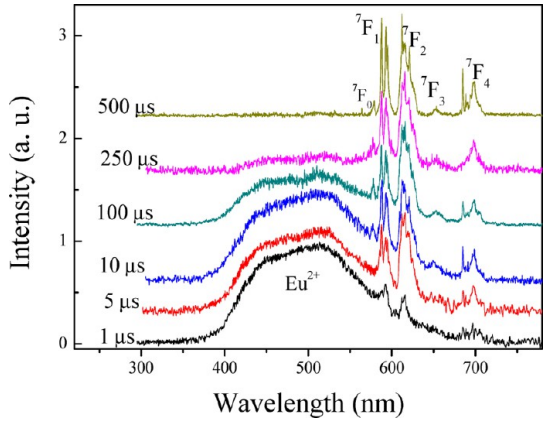


**Figure 5.** The time-resolved spectra of $CsAlSi_2O_6$:Eu prepared in air ($CsAlSi_2O_6$-A, $\lambda_{ex}$ = 266 nm) measured at different delay times after the laser excitation as labeled on the figure.


dx.doi.org/10.1021/ic402169w | Inorg. Chem. 2014, 53, 827−834

→ $^7F_{0,1,2}$ from $Eu^{3+}$ ions can be clearly observed. And the stronger $Eu^{3+}$ emission can be observed with the decrease of $Eu^{2+}$ emission by monitoring at a long delay time after laser excitation. This indicates that actually two valence states, +2, and +3, are available for Eu ions. Therefore, we can conclude that the reduction $Eu^{3+} \rightarrow Eu^{2+}$ took place in $CsAlSi_2O_6$ during the preparation in air at high temperature.

Figure 6 shows the excitation ($\lambda_{em}$ = 440, 530, or 615 nm) spectra of Eu-doped $CsAlSi_2O_6$ prepared in air. Under

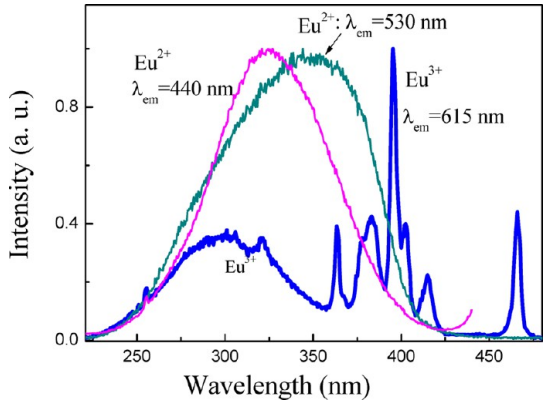


**Figure 6.** Excitation spectra of $CsAlSi_2O_6$:Eu prepared in air ($CsAlSi_2O_6$-A, $\lambda_{em}$ = 440 nm, $\lambda_{em}$ = 530 nm, and $\lambda_{em}$ = 615 nm). Each spectrum was normalized to its maximum value.

monitoring at 440 and 530 nm, an intense and broad excitation band (250- 400 nm) cantered at 350 nm can be observed, which is ascribed to the 4f−5d transition of $Eu^{2+}$ and overlaps the excitation band of the $O^{2+}$−$Eu^{3+}$ charge−transfer (CT) transition. The excitation spectrum monitored at 615 nm consists of some sharp lines belonging to transitions within the $4f^6$ configuration of $Eu^{3+}$ and a broad band from 200 to 270 nm with a maximum at about 232 nm due to the $O^{2-} \rightarrow Eu^{3+}$ CT transition. Because the PL excitation spectra show strong absorption in the range of near-UV, $CsAlSi_2O_6$:Eu could be a potential phosphor for white LEDs.[28]

The ESR spectrum of Eu-doped $CsAlSi_2O_6$ prepared in air was measured to confirm the abnormal reduction process, as shown in Figure 7. It is well-known that $Eu^{2+}$ (electronic configuration, $4f^7$; ground term, $^8S_{7/2}$) is ESR-active but $Eu^{3+}$ ($4f^6$, $^7F_0$) is ESR-inert. The pronounced ESR signal from 250 to 400 mT at effective *g*-values of 2.0 can be found in Figure 7 for

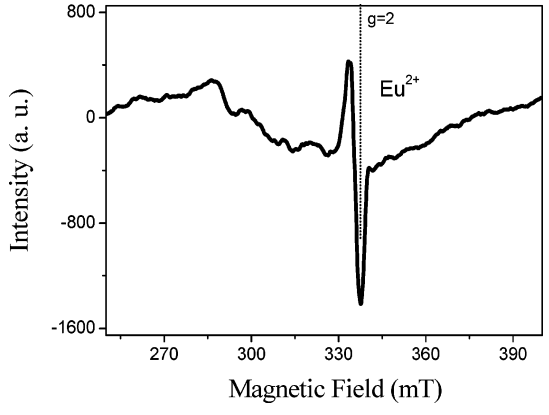


**Figure 7.** ESR signals at room temperature for Eu-doped $CsAlSi_2O_6$ prepared in air.

Eu-doped $CsAlSi_2O_6$ prepared in air. The result indicates the presence of $Eu^{2+}$ ions in the sample. On the basis of the present data, it is difficult to give a quantitative ratio of $Eu^{2+}/Eu^{3+}$ from the emission intensities of the sample because the two luminescence centers have their own characteristic excitation wavelengths.

It is obvious that the samples present different colors under different excitation wavelength because of the mixed emission components from $Eu^{2+}$ and $Eu^{3+}$. Figure 8 shows the CIE

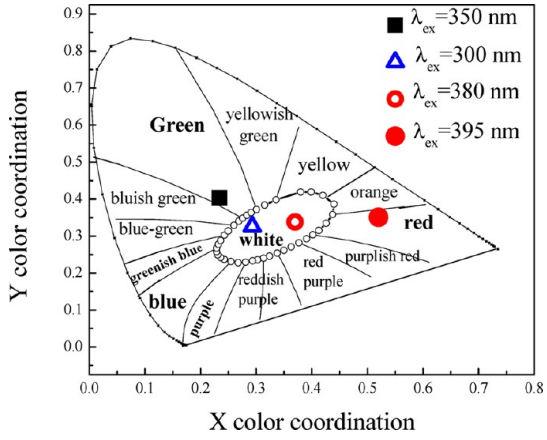


**Figure 8.** CIE chromaticity coordinates of $CsAlSi_2O_6$:Eu-A prepared in air.

(Commission Internationale de l'Ecairage 1931) chromaticity diagram calculated from the emission spectra in Figure 4. This clearly displays rich luminescence colors under the different excitation wavelengths. The sample shows green color under 350 nm, while it displays red luminescence by the excitation of 395 nm (f−f transition in $Eu^{3+}$). It is valuable that white color from a single phase in $CsAlSi_2O_6$:Eu prepared in air can be realized under the excitation of 300 and 380 nm as shown in Figure 8.

**3.3. Abnormal Reduction Mechanism of $Eu^{3+} \rightarrow Eu^{2+}$ in $CsAlSi_2O_6$.** Abnormal reductions of $RE^{3+} \rightarrow RE^{2+}$ in a compound prepared in an oxidizing atmosphere have been reported in several kinds of compounds. Four conditions are necessary to realize the abnormal reduction,[4,5,8,13,15] that is, (1) there is not oxidizing ions in the host, (2) $RE^{3+}$ (or $Eu^{3+}$) substitutes a divalent cation, (3) the substituted cation and $Eu^{2+}$ have similar radii, and (4) the host has a rigid structure, that is, having tetrahedral anion groups ($BO_4$, $SO_4$, $PO_4$, $SiO_4$, or $AlO_4$). $Eu^{3+}$-doped $CsAlSi_2O_6$ meets these conditions. And this is the first report of an abnormal reduction of $Eu^{3+}$ substituted for an alkaline metal ion, not for an alkaline earth ion.

Of the four conditions, the last one is vital for an abnormal reduction. Pollucite, $CsAlSi_2O_6$, is a member of the analcime family crystallizing in the cubic system with space group *Ia*3*d*. Figure 9 is the schematic view of the $CsAlSi_2O_6$ structure along *c*-direction. The framework is based on hexagonal and tetragonal rings of $(Si,Al)O_4$ tetrahedra as shown in Figure 9a. $Cs^+$ ions in pollucite are coordinated with 12 oxygens and arranged in the channels along [111] formed by hexagonal rings. Figure 9b displays $CsO_{12}$ polyhedra forming chains along the [111] direction. In this compound, all the O atoms are shared by the adjacent tetrahedra and all the bonds in the structure have the connection form of (Si, Al)−O−(Si, Al),[31,32] constructing a rigid aluminosilicate framework. The enclosed


dx.doi.org/10.1021/ic402169w | Inorg. Chem. 2014, 53, 827−834

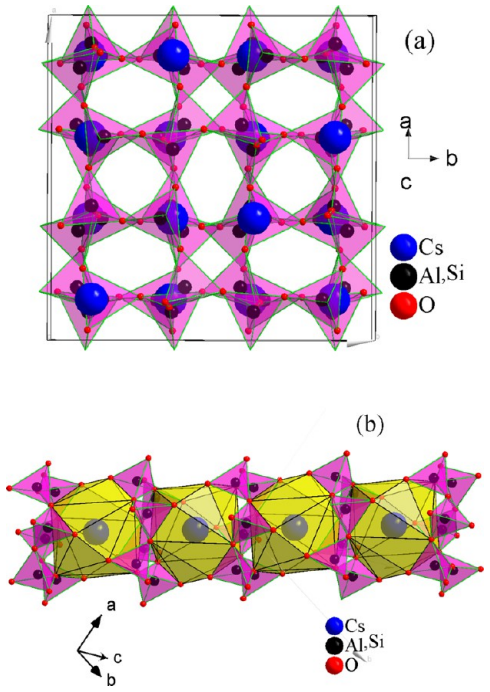


**Figure 9.** Schematic view of $CsAlSi_2O_6$ structure along *c*-direction (a) and $CsO_{12}$ chains along [111] direction (b).

and stiff three-dimensional network structure matches condition 4.

The reduction of $Eu^{3+}$ to $Eu^{2+}$ when prepared in air at high temperature can be explained by a charge compensation mechanism. To keep the electroneutrality for the substitution of $Eu^{3+}$ on $Cs^+$, a cation vacancy defect, $V_{Cs}'$, with negative charge will compensate the induced positive defects of $Eu_{Cs}^{\bullet\bullet}$, forming dipole complexes of $[(Eu^{3+}{}_{Cs})^{\bullet\bullet}-2V_{Cs}']$. The $V_{Cs}'$ would act as a donor of electrons, while $Eu_{Cs}^{\bullet\bullet}$ defects become acceptors of the electrons. Consequently, by thermal stimulation, the negative charges in the vacancy defects of $V_{Cs}'$ would be transferred to $Eu^{3+}$ sites and reduce $Eu^{3+}$ to $Eu^{2+}$. The whole process can be expressed by the following equations:

$$Eu^{3+} + 2Cs^+ \rightarrow V_{Cs}' + Eu_{Cs}^{\bullet\bullet} \quad (1)$$

$$V_{Cs}' \rightarrow V_{Cs}^{X} + e \quad (2)$$

$$Eu_{Cs}^{\bullet\bullet} + e \rightarrow Eu_{Cs}^{X} \quad (3)$$

According to the proposed reduction mechanism,[4,5,8,13,15,33,34] the tetragonal $AlO_4$ and $SiO_4$ groups in the rigid three-dimensional framework can surround and isolate the produced divalent $Eu^{2+}$ ions from reaction with oxygen.

Except for the charge compensation by cation vacancy, another mechanism related to the interstitial oxygen $O_i''$ is highly possible in $CsAlSi_2O_6$. The $O_i''$ with negative charge could be created because of the substitution of $Eu^{3+}$ on $Cs^+$, and dipole complexes of $[(Eu^{3+}{}_{Cs})^{\bullet\bullet}-O_i'']$ could be formed:

$$Eu^{3+} + Cs^+ = Eu_{Cs}^{\bullet\bullet} + O_i'' \quad (4)$$

The framework of $CsAlSi_2O_6$ consists of corner-sharing $(Si,Al)O_4$ tetrahedra arranged in four-, six-, and eight-membered rings (Figure 9a). $Cs^+$ ions occupy the cavity sites in 12-fold coordination, which are interconnected by channels through the six-member rings along [111] (Figure 9b). $SiO_4$ and $AlO_4$ tetrahedron construct a framework with enough cavities. There are ample spaces to arrange $O_i''$ to compensate the defects due to the substitution of $Eu^{3+}$ on the $Cs^+$ sites. It is not difficult to create $O_i''$ due to material preparation in air atmosphere.

Actually $O_i''$ was confirmed in $Ti^{4+}$-doped $CsAlSi_2O_6$. In $CsTi_xAl_{1-x}Si_2O_{6+0.5x}$ with $Ti^{4+}$ substituting for $Al^{3+}$ in pollucite, additional $O^{2-}$ ($O_i''$) is incorporated into the structure to maintain charge neutrality. The enthalpic variations were induced by the substitution $Ti^{4+} + 1/2O^{2-} \rightarrow Al^{3+}$ resulting in the corresponding changes in structure. As a result, the substituted $Ti^{4+}$ becomes 5-fold coordinated by oxygen in comparison with 4-fold-coordination for $Al^{3+}$. To achieve pentacoordinate geometry for every $Ti^{4+}$, the oxygen was shared by two $[TiO_5]$ pyramids via edge-sharing. The complete substitution of $Ti^{4+}$ on $Al^{3+}$ results in $CsTiSi_2O_{6.5}$.[25]

The released electron from $O_i''$ could be captured at $Eu^{3+}$ sites under a thermal stimulation resulting in the reduction of $Eu^{3+}$ to $Eu^{2+}$:

$$O_i'' \Leftrightarrow O_i' + e \quad (5)$$

$$Eu^{3+} + e \Leftrightarrow Eu^{2+} \quad (6)$$

The total defect reaction is the following, which could be expressed by $Eu^{2+}$ ions and a hole centers of $O^-$.

$$Eu^{3+} + O_i'' \Leftrightarrow [Eu^{3+} + e] + [O_i'' + h] \Leftrightarrow (Eu^{2+})^* + O_i' \quad (7)$$

In eq 7, the reduced $Eu^{2+}$ is not the same as that in eq 3, where the electrons enter into the track of the $Eu^{3+}$ ions. It could be suggested to be a kind of hydrogen-like atoms $[Eu^{3+} + e]$. However, the new measurements will be conducted in the next work to confirm the related $O^-$ ($O_i'$) hole centers.

Zhang et al.[28] suggested that $Eu^{2+}$ ions could occupy more than one site in $CsAlSi_2O_6Eu^{3+}$ lattices with luminescence centered at 440 nm ($Eu_I$) and 530 nm ($Eu_{II}$). As seen in Figure 4, the emission spectra in $CsAlSi_2O_6$-A prepared in air atmosphere have a broad band (300−600 nm) and sharp line peaks from the f−f transitions $^5D_0 \rightarrow {}^7F_J$ ($J$ = 0−4) of $Eu^{3+}$ ions. The broad spectra also have two obvious bands indicating two $Eu^{2+}$ color centers in Eu-doped $CsAlSi_2O_6$-A. In this sample, it is reasonable that $Eu^{3+}$ ions could have at least two kinds of crystallographic sites in the lattices. The multiple site structure for $Eu^{3+}$ ions doping in $CsAlSi_2O_6$-A can be understood by the charge compensation model mentioned above.

**3.4. Thermal Stability.** The temperature dependent (20−300 K) emission spectra of $CsAlSi_2O_6$-C and $CsAlSi_2O_6$-A were measured, which are shown in Figures 10 and 11, respectively. The integrated intensities of $Eu^{2+}$ emission on temperature are calculated and shown in the insets of the figures. It is observed that the emission intensity of $Eu^{2+}$ in $CsAlSi_2O_6$-C is depressed with increasing temperature from 20 to 300 K. However, the reverse phenomena can be observed in $CsAlSi_2O_6$-A, that is, $Eu^{2+}$ increases its intensity with increasing temperature from 20 to 300 K. The different stabilities on temperature for A and C should be closely related to the surrounding microstructures of $Eu^{2+}$ ions in the lattices.

During this reduction process of $Eu^{3+}$ to $Eu^{2+}$ ions in $CsAlSi_2O_6$-C, the oxygen ions surrounding $Eu^{3+}$ ions can be depleted by $H_2$ molecules when it is heated at high-temperature in ($H_2$ + $N_2$) gas.


dx.doi.org/10.1021/ic402169w | *Inorg. Chem.* 2014, 53, 827−834

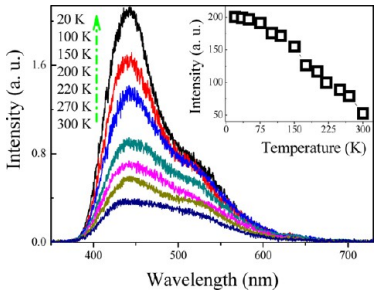


**Figure 10.** The dependence of the emission spectra of $CsAlSi_2O_6$:Eu prepared in reducing atmosphere ($CsAlSi_2O_6$-C) on the temperature 20−300 K. Inset is the total emission intensities (300−750 nm) integrated from the emission spectra.

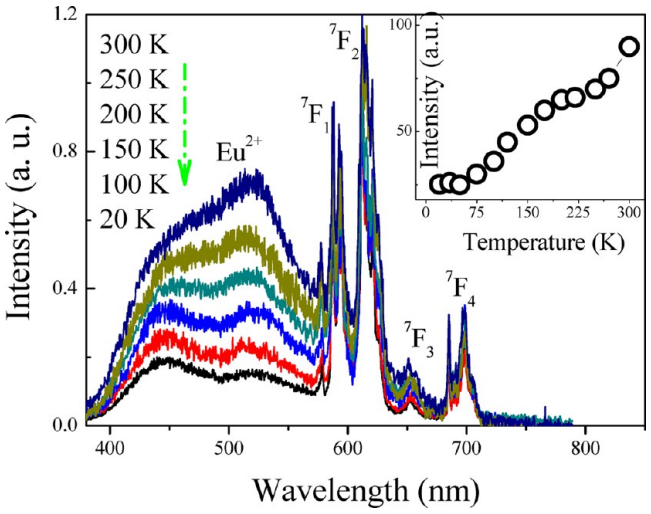


**Figure 11.** Temperature dependent emission spectra (20−300 K) of $CsAlSi_2O_6$:Eu prepared in air ($CsAlSi_2O_6$-A). Inset is the total emission intensities (300−750 nm) integrated from the emission spectra.

$$O^{2-}(\text{lattice}) + H_2(g) \rightarrow H_2O(g) + 2e \quad (8)$$

The released electrons diffuse into the crystal and complete the following reductive reaction of trivalent $Eu^{3+}$.

$$Eu^{3+}[Xe]4f^5 + e \rightarrow Eu^{2+}[Xe]4f^6 \quad (9)$$

The electron comes into the atom track of $Eu^{2+}$. The enhancement of luminescence with decreasing temperature is due to weak electron−phonon interaction at low temperature.

However, the reduction of $Eu^{3+}$ to $Eu^{2+}$ in $CsAlSi_2O_6$-A is a different mechanism from that in $CsAlSi_2O_6$-C. There are two possible defect traps of $[(Eu^{3+}_{Cs})^{\bullet\bullet}-O_i'']$ or $[(Eu^{3+}_{Cs})^{\bullet\bullet}-2V_{Cs}']$ in $CsAlSi_2O_6$-A. $Eu^{2+}$ ions could be recombined with the electrons released from defects $O_i''$ or $V_{Cs}'$; however, the electrons do not enter the atom track of $Eu^{2+}$ but loosely combine with $Eu^{3+}$ in close vicinity ($Eu^{3+}$ + e) presenting luminescence of $Eu^{2+}$ under excitation. So the different defect traps in the matrix should be attributed to the mechanisms of $Eu^{3+}$ to $Eu^{2+}$ ions. With decreasing temperature, all the defects could be inert at low temperature and resulting in low luminescence of $Eu^{2+}$ ion.

The decay curves of $Eu^{2+}$ emission centers in $CsAlSi_2O_6$-C and $CsAlSi_2O_6$-A are displayed in Figures 12 and 13, respectively. The lifetime shows some quenching from 20 to 300 K. It can be found that the lifetimes of $Eu^{2+}$ emission

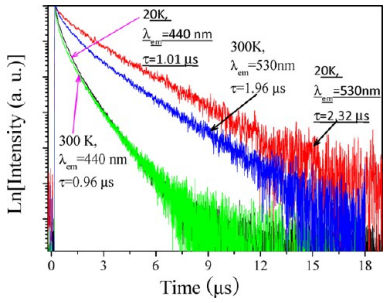


**Figure 12.** Decay curves of $Eu^{2+}$ centers at 440 and 530 nm in $CsAlSi_2O_6$-C at 20 and 300 K.

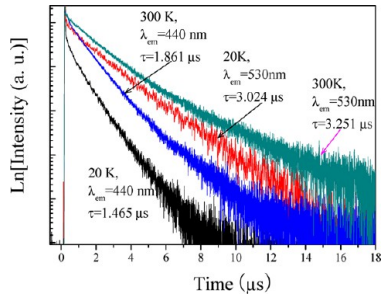


**Figure 13.** Decay curves of $Eu^{2+}$ centers 440 and 530 nm in $CsAlSi_2O_6$-A at 20 and 300 K.

centers in $CsAlSi_2O_6$ show the unusual increase from 20 to 300 K; this deviates the well-known fact that the lifetimes of $Eu^{2+}$ excited states usually decrease with temperature enhancement. Similar abnormal decrease of lifetime with increasing temperature has been reported in $Eu^{2+}$-doped $CaF_2$,[35,36] $Ba_5SiO_4X_6$ (X = Cl or Br),[37] and BaFBr[38] from 10 K to room temperature. This is a really complicated process, which was assigned to different mechanisms. In $Eu^{2+}$-doped $CaF_2$ the increase of lifetime with increasing temperature was ascribed to the existence of states with lower oscillator strength lying above the lowest excited level.[35] The excited state $^6P_J$ produced by the $f^7$ electron configuration of the $Eu^{2+}$ ion is located above the lowest excited state produced by the $f^6d$ configuration. However, Tsuboi et al.[36] suggested that that two relaxed excited states (RESS) were responsible for the blue emission in $CaF_2$:$Eu^{2+}$. The low-energy RES I is related to the lowest excited state of the $f^6d$ configuration, while the upper RES II is produced by the excited state of the $f^7$ configuration. The transition from the RES II is forbidden. Consequentially, the transition was delayed at higher temperature. In $Eu^{2+}$-$Ba_5SiO_4X_6$ (X = Cl or Br) Meijerink et al.[37] explained the unusual increase by the thermal population of higher energetic $4f^65d$ for which the transition probability to $4f^7$ ($^8S^{7/2}$) ground states was smaller than for the lowest $4f^65d$ state. At present, it is still difficult to assign which is the real mechanism for $Eu^{2+}$-doped $CsAlSi_2O_6$ because of the multiple site structure for $Eu^{2+}$ ions in $CsAlSi_2O_6$.[28] The further work will be needed for the detailed crystallographic information.

It is well-known that in a system with two luminescence centers energy transfer could take place from the high-energy centers to another with a low energy level. For example, in the $Ba_3LaNa(PO_4)_3F$:$Eu^{2+}$,$Tb^{3+}$ phosphor, the blue emission (425−525 nm) of $Eu^{2+}$ ions can be efficiently transferred to the low-energy-lying $Tb^{3+}$ ions resulting in bright blue-green or pure green color.[39] In $Eu^{2+}$ and $Eu^{3+}$ codoped KCl, an


dx.doi.org/10.1021/ic402169w | Inorg. Chem. 2014, 53, 827−834

extraordinary emission feature can be produced via the process of energy reabsorption from $Eu^{2+}$ to $Eu^{3+}$ ions.[40] At all temperatures, the predominant emission is from the $^5D_0 \rightarrow {}^7F_2$ transitions of $Eu^{3+}$ ions. In addition, the broad emission of $Eu^{2+}$ overlaps the sharp excitation peaks originating from the f−f transition of $Eu^{3+}$. It is possible that energy transfer would occur from $Eu^{2+}$ to $Eu^{3+}$. This kind of energy transfer could also take place in the sample with increasing or decreasing temperature; the detailed precess is not clear. The main problem is that there are at least two kinds of luminescence for $Eu^{2+}$ and $Eu^{3+}$ in the sample lattices, and the detailed energy level diagram of the $Eu^{2+}$ and $Eu^{3+}$ ions in this crystal will be investigated in further work.

Figure 14 displays the decay curves of $Eu^{3+}$ emission in the $CsAlSi_2O_6$-A sample at several temperatures; the lifetimes of

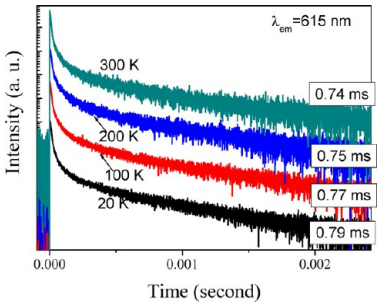


**Figure 14.** Decay curves of $Eu^{3+}$ emission in $CsAlSi_2O_6$-A sample at selected temperature from 20 to 300 K.

$Eu^{3+}$ do not show obvious change at different temperatures (i.e., 20 and 300 K). This indicates that the luminescence of $Eu^{3+}$ in the $CsAlSi_2O_6$ host has high thermal stability. This can benefit lighting and display applications.

## 4. CONCLUSIONS

Eu-doped $CsAlSi_2O_6$ was prepared by the sol−gel method and finally heated in air atmosphere at 1300 °C. The emission spectra of $CsAlSi_2O_6$:Eu prepared in air present the broad band of $Eu^{2+}$ and sharp emission lines corresponding to the $^5D_0-{}^7F_J$ ($J$ = 0, 1, 2, 3, and 4) transitions of $Eu^{3+}$. There are two valence states, +2 and +3, available for Eu ions. The time-resolved spectra can distinctly separate the $Eu^{3+}$ luminescence from that of $Eu^{2+}$ ions. This abnormal reduction $Eu^{3+} \rightarrow Eu^{2+}$ is closely related to the charge compensation mechanism and a rigid three-dimensional framework structure of $CsAlSi_2O_6$ containing tetrahedral anion groups, $(Si,Al)O_4$. The substitution of $Eu^{3+}$ on $Cs^+$ can induce possible defect complexes of $[(Eu^{3+}{}_{Cs})^{\bullet\bullet}-2V_{Cs}{}']$ or $[(Eu^{3+}{}_{Cs})^{\bullet\bullet}-O_i{}'']$. In $Eu^{2+}$-doped $CsAlSi_2O_6$ prepared in reducing atmospheres, released electrons comes into the atom track of $Eu^{2+}$, resulting in complete reduction of $Eu^{3+}$ to $Eu^{2+}$ ions. This sample presents a luminescence enhancement with decreasing temperature due to weak electron−phonon interaction at low temperature. However, in $Eu^{2+}$-doped $CsAlSi_2O_6$ with an abnormal reduction, $Eu^{2+}$ ions could be obtained by just loosely combining the released electrons from defects $O_i{}''$ or $V_{Cs}{}'$; the electrons could be in close vicinity of $Eu^{3+}$ ($Eu^{3+}$ + e) and not enter the atom track of $Eu^{2+}$. This complex presents luminescence of $Eu^{2+}$ ions. With decreasing temperature, all the defects could be inert at low temperature and resulting in decrease of luminescence of $Eu^{2+}$ ion. So different defect traps are attributed to the abnormal reduction mechanism of $Eu^{3+}$ to $Eu^{2+}$ ions in a matrix.

## AUTHOR INFORMATION

### Corresponding Author

*E-mail: hjseo@pknu.ac.kr (Hyo Jin Seo). Tel: +82-51-629 5568. Fax:+82-51-6295549.

### Notes

The authors declare no competing financial interest.

## ACKNOWLEDGMENTS

This research was supported by Basic Science Research Program through the National Research Foundation of Korea (NRF) funded by the Ministry of Science, ICT & Future Planning (NRF-2013R1A1A2009154), and by a project funded by the Priority Academic Program Development of Jiangsu Higher Education Institutions (PAPD).

## REFERENCES

(1) Pei, Z.; Su, Q.; Zhang, J. *J. Alloys Compd.* **1993**, *198*, 51−53.
(2) Su, Q.; Liang, H.; Hu, T.; Tao, Y.; Liu, T. *J. Alloys Compd.* **2002**, *344*, 132−136.
(3) Hao, J. H.; Gao. *J. Appl. Phys. Lett.* **2004**, *85*, 3720−3723.
(4) Pei, Z.; Zeng, Q.; Su, Q. *J. Solid State Chem.* **1999**, *145*, 212−215.
(5) Pei, Z.; Zeng, Q.; Su, Q. *J. Phys. Chem. Solids* **2000**, *61*, 9−12.
(6) Peng, M.; Pei, Z.; Hong, G.; Su, Q. *Chem. Phys. Lett.* **2003**, *371*, 1−6.
(7) Zeng, Q. H.; Pei, Z. W.; Wang, S. B.; Su, Q. *Chem. Mater.* **1999**, *11*, 605−611.
(8) Peng, M. Y.; Hong, G. Y. *J. Lumin.* **2007**, *127*, 735−740.
(9) Täle, I.; Külis, P.; Kronghauz, V. *J. Lumin.* **1979**, *20*, 343−347.
(10) Grandhe, B. K.; Bandi, V. R.; Jang, K. W.; Kim, S. S.; Shin, D. S.; Lee, Y. I.; M Lim, J.; Song, T. K. *J. Alloys Compd.* **2011**, *509*, 7937−7942.
(11) Jing, H. Q.; Wu, G. Q.; Du, B. S. *Chem. J. Chin. Univ.* **1997**, 181425.
(12) Su, Q.; Liang, H. B.; Hu, T. D.; Tao, Y.; Liu, T. *J. Alloys Compd.* **2002**, *344*, 132−136.
(13) Peng, M. Y.; Pei, Z. W.; Hong, G. Y.; Su, Q. *J. Mater. Chem.* **2003**, *13*, 1202−1205.
(14) Madhusoondanan, U.; Jose, M. T.; Lakshmanan, A. R. *Radiat. Meas.* **1999**, *30*, 65.
(15) Lian, Z. H.; Wang, J.; Lv, Y. H.; Wang, S. B.; Su, Q. *J. Alloys Compd.* **2007**, *430*, 257−261.
(16) Zhang, Q.; Liu, X. F.; Qiao, Y. B.; Qian, B.; Dong, G. P.; Ruan, J.; Zhou, Q. L.; Qiu, Ji. R.; Chen, D. P. *Opt. Mater.* **2010**, *32*, 427−431.
(17) Yanagisawa, K.; Nishioka, M.; Yamasaki, N. *J. Nucl. Sci. Technol.* **1987**, *24*, 51−60.
(18) Komameni, S.; White, W. B. *Sci. Basis Nucl. Waste Manage.* **1981**, *3*, 387−396.
(19) Mimura, H.; Shibata, M.; Akiba, K. *J. Nucl. Sci. Technol.* **1990**, *27*, 835−843.
(20) Taylor, D.; Henderson, C. M. B. *Am. Mineral.* **1968**, *55*, 1476−1489.
(21) Richerson, D. W.; Hummel, F. A. *J. Am. Ceram. Soc.* **1972**, *55*, 269−273.
(22) Kobayashi, H.; Yanase, I.; Mitamura, T. *J. Am. Ceram. Soc.* **1997**, *80*, 2161−2164.
(23) Teertstra, D. K.; Sherriff, B. L.; Xu, Z.; Cerny, P. *Can. Miner.* **1994**, *32*, 69−80.
(24) Xu, H. W.; Navrotsky, A.; Balmer, M. L.; Su, Y. L.; Bitten, E. R. *J. Am. Ceram. Soc.* **2001**, *84*, 555−560.
(25) MacLaren, I.; Cirre, J.; Ponton, C. B. *J. Am. Ceram. Soc.* **1999**, *82*, 3242−3244.
(26) Ogorodova, L. P.; Melchakova, L. V.; Kiseleva, I. A.; Belitsky, I. A. *Thermochim. Acta* **2003**, *403*, 251−256.
(27) Montagna, G.; Arletti, R.; Vezzalini, G.; Renzo, F. D. *Powder Technol.* **2011**, *208*, 491−495.
(28) Zhang, W. S.; Wei, D. L.; Seo, H. J. *Mater. Lett.* **2013**, *94*, 140−142.

(29) Nogami, M.; Yamazaki, T.; Abe, Y. *J. Lumin.* **1998**, *78*, 63−68.
(30) Blasse, G.; Grabmarier, B. C. *Luminescence Materials*; Springer: Berlin, Heidelberg, 1994; p 41.
(31) Loginova, E. E.; Orlova, A. I. D.; Mikhailov, A.; Troshin, A. N.; Borovikova, E. Yu.; Samoilov, S. G.; Kazantsev, G. N.; Kazakova, A. Yu.; Demarin, V. T. *Radiochemistry* **2011**, *53*, 593−603.
(32) Yanase, I.; Kobayashi, H.; Shibasaki, Y.; Mitamura, T. *J. Am. Ceram. Soc.* **1997**, *80*, 2693−2695.
(33) Su, Q.; Zeng, Q. H.; Pei, Z. W. *Chin. J. Inorg. Chem.* **2000**, *16*, 293−298.
(34) Machida, K.; Adachi, G.; Shiokawa, J. *Acta Crystallogr.* **1980**, *B36*, 2008−2011.
(35) Kisliuk, P.; Tippins, H. H.; Moore, C. A.; Pollack, S. A. *Phys. Rev.* **1968**, *171*, 336−342.
(36) Tsuboi, T.; Silfsten, P. *J. Phys.: Condensed Matter* **1991**, *3*, 9163.
(37) Meijerink, A.; Blasse, G. *J. Lumin.* **1990**, *47*, 1−5.
(38) Spoonhower, J. P.; Burberry, M. S. *J. Lumin.* **1989**, *43*, 221.
(39) Jiao, M.; Guo, N.; Lü, W.; Jia, Y.; Lv, W.; Zhao, Q.; Shao, B.; You, H. *Inorg. Chem.* **2013**, *52*, 10340−10346.
(40) Kang, J. G.; Nah, M. K.; Sohn, Y. *J. Phys.: Condens. Matter* **2000**, *12*, L199−L203.